*Korean J. Chem. Eng.*, **24**(3), 379-390 (2007)

# Controlled output variance based diagnosis tree for feedforward/cascade control systems

**Junghui Chen**† **and Cho-Kai Kong**

R&D Center for Membrane Technology and Department of Chemical Engineering,
Chung-Yuan Christian University, Chung-Li, Taiwan 32023, Republic of China
(*Received 11 July 2006 • accepted 6 November 2006*)

**Abstract**−This paper aims at providing a framework for detection and diagnosis of the performance of a combinational feedforward (FF) and cascade (CC) control system. It is the extension of our previous work [1,2]. The main idea is to extract the only CC effect and the combination of FF with CC effects, respectively. In the only CC effect, the output variances of the primary and the secondary loops can be turned into the cascade-invariant and cascade-dependent terms, respectively. The combination of FF with CC effect can also be decomposed into the cascade/feedforward invariant term, the cascade-invariant/feedforward-dependent term and the cascade/feedforward dependent term. The diagnosis tree based on these decomposition terms is proposed to assess the performance of the FF/CC control system. The sequence of the statistical inference system is developed to diagnose fault causes. The capability of the proposed method is demonstrated via a cascade control system with the feedforward loops and multiple faults.

Key words: Cascade Control, Control Loop Performance, Feedforward Control, Monitoring and Diagnosis

## INTRODUCTION

Performance monitoring methods of chemical plants can considerably help obtain upgraded and condensed information from the operation control system to support process safety, operation profitability, and delivery of consistently high quality, etc. It is particularly important as the complexity of chemical process systems has increased. The regular estimation of the control performance can be used to monitor and evaluate how likely it is to improve control performance [3]. The most common techniques are the stochastic minimum-variance methods whose current control performance is compared to a type of achievable performance, minimum variance control. A variety of control applications based on the minimum variance benchmark have been developed, including feedback control [4], feedforward/feedback control [5], multiloop control [6], model-based control [7], and cascade control [8,9].

The performance assessment using the minimum variance control (MVC) is attractive as it is easy to use. Also, it requires only normal, closed-loop operation data and knowledge of the process time delay. However, assessing whether current output variance is significantly deviated from the benchmark variance only shows the current performance monitoring. It only indicates the poor performance in the control loop. It does not find out and remove the fault causes associated with the performance degradation. The degraded performance may come from severe disturbance changes or a significant change in the dynamic plant characteristics. If the deterioration of the controlled performance cannot be identified in time, unwanted variances would prevent the operating processes from achieving their true process capability. Stanfelj et al. [10] monitored the cause of the poor performance of the feedback and the feedforward system via a decision tree structure with small perturbation in the setpoint. A data-driven method combined with the prior process knowledge was applied to exploring the root cause [11]. Yea and Chen [1,2] divided the controlled output variance into the controller invariant term and the controller dependent term for a feedback control system and a feedforward control system. Then the statistical inference is applied to the above two terms to build up a diagnostic reasoning tree that could locate and remove the root causes.

This article focuses on the combinational feedforward (FF) and cascade (CC) control loop. The control structure is often used in the propene rectification tower of a naphtha cracking plant. The combination of FF and CC control is often used to eliminate the loss of the high value of propene in the outlet of the C3LPG stream. The FF controller rejects the inlet of the feed flow rate disturbances. The disturbances directly affecting the product quality are compensated by cascading the composition controller to a C3LPG flow controller. The secondary controller of the inner loop allows rapid rejection or reduction of the steam pressure disturbances before the disturbances effects spill over to the composition control of the primary loop, resulting in little effect on the output composition. Although the combination of the FF and CC control structure is commonly used in industries, the control performance has not yet been evaluated. In this paper a methodology for the performance detection and diagnosis of the FF/CC control structure is developed. Like the performance analysis of the feedback control [10], the primary and the secondary output variances of the FF/CC control structure can be separated into the controller invariant terms and the controller dependent terms, respectively. Any fault in the FF/CC control loops might affect either or both of the controller invariant terms and the controller dependent terms of the primary and the secondary output variances for the unmeasured disturbances and the measured disturbances. Using these terms as performance fingerprints, a new diagnostic methodology for the FF/CC control system is proposed. The rest of the paper is structured as follows. The second section defines the diagnosis problem of the feedforward/cascade control (FF/CC) system. The proposed fault diagnosis method is based on the output variation, and the performance assessment of FF/CC sys-

†To whom correspondence should be addressed.
E-mail: jason@wavenet.cycu.edu.tw

tem is also derived. Then the diagnostic reasoning tree of FF/CC using impulse response analysis to detect the fault sources is derived in Section 3. A simulation cascade control system with two feedforward loops is demonstrated to explore the diagnosis of the more complex control structure based on the controlled output variances in Section 4. Finally, the conclusions are made.

## PERFORMANCE BOUND OF FEEDFORWARD/CASCADE SYSTEMS

The block diagram of a FF/CC control system shown in Fig. 1 consists of a cascade control with multiple feedforward variables. The cascade control structure has two control loops. The inner (or the secondary) loop is embedded within an outer (or primary) loop. $y_1(k)$ and $y_2(k)$ are the process outputs of the primary and the secondary loops at the sampling time k. The process contains two components $G_{P_1}(k)$ and $G_{P_2}(k)$. $G^u_{L_1}(k)$ and $G^u_{L_2}(k)$ are unmeasured disturbances ($w^u_1(k)$ and $w^u_2(k)$) to the primary output and the secondary output, respectively. The goal of CC is to make $y_1(k)$ reach the set point as long as there are constraints on $y_2(k)$. The inner-loop controller, $G^{cc}_{C_2}(k)$, is used to regulate the constrained output $y_2(k)$. $G^{cc}_{C_2}(k)$ is tuned to avoid overshooting of the constrained variable $y_2(k)$. The outer-loop controller, $G^{cc}_{C_1}(k)$, is tuned to regulate the output $y_1(k)$ to its set point. $G^m_{L_1,j}(k)$, j=1, 2, …, M and $G^m_{L_2,i}(k)$, i=1, 2, …, N are measured disturbances to the primary and the secondary output, respectively. The goal of FF controllers ($G^{ff}_{C_1,j}$, j=1, 2, …, M and $G^{ff}_{C_2,i}$, i=1, 2, …, N) is to compensate for entering measured disturbances from the primary loop ($w^m_{1,j}(k)$, j=1, 2, …, M) and from the secondary loop ($w^m_{2,i}(k)$, i=1, 2, …, N). Here the disturbances are a sequence of zero mean independent distribution with constant variance. $u_1(k)$ and $u_2(k)$ are the controller outputs of $G^{cc}_{C_1}(k)$ and $G^{cc}_{C_2}(k)$. When the primary setpoint is constant, the closed-loop responses ($\{y_1(k)\}$ and $\{y_2(k)\}$) to the unmeasured disturbances, and the measured disturbances from the secondary loop and from the primary loop can be derived as

$$
\begin{aligned}
y_1 &= y_{1,CC} + y_{1,FF} \\
&= \underbrace{\frac{(1+G_{P_2}G^{cc}_{C_2})G^u_{L_1}}{1+G_{P_2}G^{cc}_{C_2}+G_{P_1}G_{P_2}G^{cc}_{C_1}G^{cc}_{C_2}}}_{Cascade} w^u_1 \\
&\quad + \underbrace{\frac{G_{P_1}G^u_{L_2}}{1+G_{P_2}G^{cc}_{C_2}+G_{P_1}G_{P_2}G^{cc}_{C_1}G^{cc}_{C_2}}}_{Cascade} w^u_2 \\
&\quad + \sum_{j=1}^{M} \underbrace{\frac{G^m_{L_1,j}+G^m_{L_1,j}G_{P_2}G^{cc}_{C_2}+G_{P_1}G_{P_2}G^{ff}_{C_1,j}}{1+G_{P_2}G^{cc}_{C_2}+G_{P_1}G_{P_2}G^{cc}_{C_1}G^{cc}_{C_2}}}_{Cascade/Feedforward} w^m_{1,j} \\
&\quad + \sum_{i=1}^{N} \underbrace{\frac{G_{P_1}(G^m_{L_2,i}+G_{P_2}G^{ff}_{C_2,i})}{1+G_{P_2}G^{cc}_{C_2}+G_{P_1}G_{P_2}G^{cc}_{C_1}G^{cc}_{C_2}}}_{Cascade/Feedforward} w^m_{2,i}
\end{aligned} \tag{1}
$$

$$
\begin{aligned}
y_2 &= y_{2,CC} + y_{2,FF} \\
&= \underbrace{\frac{-G_{P_2}G^{cc}_{C_1}G^{cc}_{C_2}G^u_{L_1}}{1+G_{P_2}G^{cc}_{C_2}+G_{P_1}G_{P_2}G^{cc}_{C_1}G^{cc}_{C_2}}}_{Cascade} w^u_1 \\
&\quad + \underbrace{\frac{G^u_{L_2}}{1+G_{P_2}G^{cc}_{C_2}+G_{P_1}G_{P_2}G^{cc}_{C_1}G^{cc}_{C_2}}}_{Cascade} w^u_2 \\
&\quad + \sum_{j=1}^{M} \underbrace{\frac{G_{P_2}G^{ff}_{C_1,j}-G_{P_2}G^{cc}_{C_1}G^{cc}_{C_2}G^m_{L_1,j}}{1+G_{P_2}G^{cc}_{C_2}+G_{P_1}G_{P_2}G^{cc}_{C_1}G^{cc}_{C_2}}}_{Cascade/Feedforward} w^m_{1,j} \\
&\quad + \sum_{i=1}^{N} \underbrace{\frac{G^m_{L_2,i}+G_{P_2}G^{ff}_{C_2,i}}{1+G_{P_2}G^{cc}_{C_2}+G_{P_1}G_{P_2}G^{cc}_{C_1}G^{cc}_{C_2}}}_{Cascade/Feedforward} w^m_{2,i}
\end{aligned} \tag{2}
$$

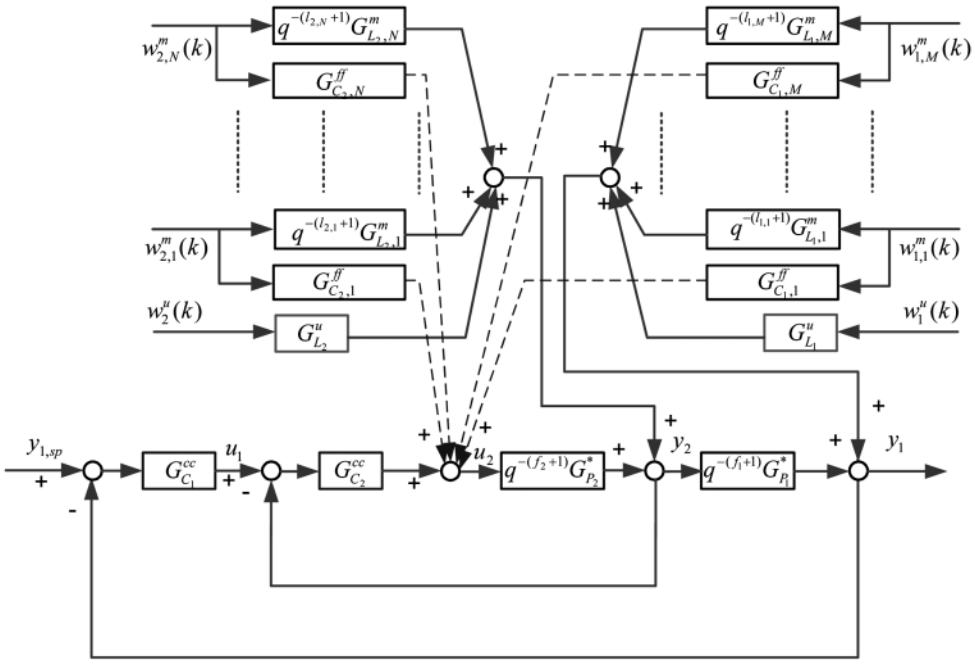


**Fig. 1. A cascade control/feedforward system.**

The detection and diagnosis procedures will analyze the measured output data ($y_1(k)$ and $y_2(k)$) and find out the fault causes when the process faults occur. Assume $G_{P_1}$ and $G_{P_2}$ can be represented by $G_{P_1}=G^*_{P_1}q^{-(f_1+1)}$ and $G_{P_2}=G^*_{P_2}q^{-(f_2+1)}$, where $f_i$, i=1, 2, are the time delays and $G^*_{P_i}$, i=1, 2 are the process models without any time delay. Also, $G^m_{L_1,j}$ and $G^m_{L_2,i}$ are represented by $G^m_{L_1,j}=(G^m_{L_1,j})^* q^{-(l_{1,j}+1)}$ and $G^m_{L_2,i}=(G^m_{L_2,i})^* q^{-(l_{2,i}+1)}$, where $l_{1,j}$ and $l_{2,i}$ are the time delays of the measured disturbances, and $(G^m_{L_1,j})^*$ j=1, 2, …, M and $(G^m_{L_2,i})^*$ i=1, 2, …, N are the measured disturbance models without any time delay. The above models are replaced by the following polynomial division identities,

$$
\begin{aligned}
&G^u_{L_1}= Q^u_1 + R^u_1 q^{-(f_1+f_2+2)}\\
&G^u_{L_2}= Q^u_2 + R^u_2 q^{-(f_2+1)}\\
&(G^m_{L_1,j})^* = Q^m_{1,j} + R^m_{1,j} q^{-(f_1+f_2+2)} \qquad \text{where j=1, 2, …, M}\\
&(G^m_{L_2,i})^* = Q^m_{2,i} + R^m_{2,i} q^{-(f_2+1)} \qquad \text{where i=1, 2, …, N}\\
&G^*_{P_1} Q^u_2 = E + F q^{-(f_2+1)}\\
&G^*_{P_2} Q^u_1 = G + H q^{-(f_1+1)}\\
&G^*_{P_2} Q^m_{1,j} = I_{1,j} + J_{1,j} q^{-(f_1+1)} \qquad \text{where j=1, 2, …, M}\\
&G^*_{P_1} Q^m_{2,i} = K_{2,i} + L_{2,i} q^{-(f_2+1)} \qquad \text{where i=1, 2, …, N}
\end{aligned}
\tag{3}
$$

Eq. (3) is called Diophantine equations. $Q^u_1$ and $Q^u_2$ are polynomials of degree $f_1+f_2+1$ and $f_2$, respectively; $Q^m_{1,j}$ and $Q^m_{2,i}$ are polynomials of degree $f_1+f_2+1$ and $f_2$, respectively; $R^u_1$, $R^u_2$, $R^m_{1,j}$ and $R^m_{2,i}$ are proper transfer functions. Substituting the identities in Eq. (3) into Eqs. (1)-(2), the outputs ($y_1(k)$ and $y_2(k)$) can be expressed as

$$
\begin{aligned}
y_1 &= y_{1,CC} + y_{1,FF}\\
&= \left[ \underbrace{Q^u_1}_{CI_{11}} + \underbrace{q^{-(f_1+f_2+2)} S(R^u_1 + G^*_{P_2} G^{cc}_{C_2} R^u_1 + G^*_{P_1} G^*_{P_2} G^{cc}_{C_1} G^{cc}_{C_2} Q^u_1)}_{CD_{11}} \right] w^u_1\\
&\quad + \left[ \underbrace{q^{-(f_1+1)} E}_{CI_{12}} + \underbrace{\begin{array}{l} q^{-(f_1+f_2+2)} S((F + G^*_{P_2} R^u_2)\\ - G^*_{P_2} G^{cc}_{C_2} E + G_{P_1} G^*_{P_2} G^{cc}_{C_1} G^{cc}_{C_2} E) \end{array}}_{CD_{12}} \right] w^u_2\\
&\quad + \left\{ \begin{array}{l}
\sum_{j=1}^{M} \left[ \underbrace{q^{-(l_{1,j}+1)} Q^m_{1,j}}_{CI/FFI} + \underbrace{q^{-(f_1+f_2+2)} G^*_{P_1} G^*_{P_2} G^{ff}_{C_{1,j}}}_{CI/FFD} \right.\\
\quad + \underbrace{q^{-(f_1+f_2+l_{1,j}+3)} S(R^m_{1,j} - G^*_{P_1} G^*_{P_2} G^{cc}_{C_1} G^{cc}_{C_2} Q^m_{1,j} + G_{P_2} G^{cc}_{C_2} R^m_{1,j})}_{CD/FFD}\\
\quad \left. - \underbrace{\begin{array}{l} q^{-(f_1+f_2+2)} S(q^{-(f_2+1)} G^*_{P_1} (G^*_{P_2})^2 G^{cc}_{C_2} G^{ff}_{C_{1,j}}\\ + q^{-(f_1+f_2+2)} (G^*_{P_1})^2 (G^*_{P_2})^2 G^{cc}_{C_1} G^{cc}_{C_2} G^{ff}_{C_{1,j}}) \end{array}}_{CD/FFD} \right] w^m_{1,j} \qquad \text{if } l_{1,i} < f_1 + f_2\\
\sum_{j=1}^{M} \left[ \underbrace{q^{-(f_1+f_2+2)} G^*_{P_1} G^*_{P_2} G^{ff}_{C_{1,j}}}_{CI/FFD} \right.\\
\quad + \underbrace{q^{-(f_1+f_2+l_{1,j}+3)} S(R^m_{1,j} - G^*_{P_1} G^*_{P_2} G^{cc}_{C_1} G^{cc}_{C_2} Q^m_{1,j} + G_{P_2} G^{cc}_{C_2} R^m_{1,j})}_{CD/FFD}\\
\quad \left. - \underbrace{\begin{array}{l} q^{-(f_1+f_2+2)} S(q^{-(f_2+1)} G^*_{P_1} (G^*_{P_2})^2 G^{cc}_{C_2} G^{ff}_{C_{1,j}}\\ + q^{-(f_1+f_2+2)} (G^*_{P_1})^2 (G^*_{P_2})^2 G^{cc}_{C_1} G^{cc}_{C_2} G^{ff}_{C_{1,j}}) \end{array}}_{CD/FFD} \right] w^m_{1,j} \qquad \text{if } l_{1,i} \geq f_1 + f_2
\end{array} \right\}\\
&\quad + \left\{ \begin{array}{l}
\sum_{i=1}^{M} \left[ \underbrace{q^{-(f_1+l_{2,i}+2)} K_{2,i}}_{CI/FFI} + \underbrace{q^{-(f_1+f_2+2)} G^*_{P_1} G^*_{P_2} G^{ff}_{C_{2,i}}}_{CI/FFD} \right.\\
\quad + q^{-(f_1+f_2+l_{2,i}+3)} S(L_{2,i} + G^*_{P_1} R^m_{L_{2,i}} - K_{2,i} G^*_{P_2} G^{cc}_{C_2}\\
\quad \underbrace{+ q^{-(f_1+1)} K_{2,i} G^*_{P_1} G^*_{P_2} G^{cc}_{C_1} G^{cc}_{C_2})}_{CD/FFD}\\
\quad \left. - \underbrace{\begin{array}{l} q^{-(f_1+f_2+2)} S(G^*_{P_1} (G^*_{P_2})^2 G^{ff}_{C_{2,i}} G^{cc}_{C_2}\\ + q^{-(f_1+1)} (G^*_{P_1})^2 (G^*_{P_2})^2 G^{ff}_{C_{2,i}} G^{cc}_{C_1} G^{cc}_{C_2} \end{array}}_{CD/FFD} \right] w^m_{2,i} \qquad \text{if } l_{2,i} < f_2\\
\sum_{i=1}^{M} \left[ \underbrace{q^{-(f_1+f_2+2)} G^*_{P_1} G^*_{P_2} G^{ff}_{C_{2,i}}}_{CI/FFD} \right.\\
\quad + q^{-(f_1+f_2+l_{2,i}+3)} S(L_{2,i} + G^*_{P_1} R^m_{L_{2,i}} - K_{2,i} G^*_{P_2} G^{cc}_{C_2}\\
\quad \underbrace{+ q^{-(f_1+1)} K_{2,i} G^*_{P_1} G^*_{P_2} G^{cc}_{C_1} G^{cc}_{C_2})}_{CD/FFD}\\
\quad \left. - \underbrace{\begin{array}{l} q^{-(f_1+2f_2+3)} S(G^*_{P_1} (G^*_{P_2})^2 G^{ff}_{C_{2,i}} G^{cc}_{C_2}\\ + q^{-(f_1+1)} (G^*_{P_1})^2 (G^*_{P_2})^2 G^{ff}_{C_{2,i}} G^{cc}_{C_1} G^{cc}_{C_2} \end{array}}_{CD/FFD} \right] w^m_{2,i} \qquad \text{if } l_{2,i} \geq f_2
\end{array} \right\}
\end{aligned}
\tag{4}
$$

$$
\begin{aligned}
y_2 &= y_{2,CC} + y_{2,FF}\\
&= \left[ \underbrace{q^{-(f_2+1)} S(G G^{cc}_{C_1} G^{cc}_{C_2} + q^{-(f_1+1)} G^{cc}_{C_1} G^{cc}_{C_2} H + q^{-(f_1+f_2+2)} G^*_{P_2} G^{cc}_{C_1} G^{cc}_{C_2} R^u_1)}_{CD_{21}} \right] w^u_1\\
&= \left[ \underbrace{Q^u_2}_{CI_{22}} + \underbrace{q^{-(f_2+1)} S(R^u_2 - G^*_{P_2} G^{cc}_{C_2} Q^u_2 - q^{-(f_1+1)} G^*_{P_1} G^*_{P_2} G^{cc}_{C_1} G^{cc}_{C_2} Q^u_2)}_{CD_{22}} \right] w^u_2\\
&\quad + \left\{ \begin{array}{l}
\sum_{j=1}^{M} \left[ \underbrace{z^{-(f_2+1)} G^*_{P_2} G^{ff}_{C_{1,j}}}_{CI/FFD} \right.\\
\quad + \underbrace{q^{-(f_2+l_{1,j}+2)} S(G^{cc}_{C_1} G^{cc}_{C_2} I_{1,1} + q^{-(f_1+1)} G^{cc}_{C_1} G^{cc}_{C_2} J_{1,j} + q^{-(f_1+f_2+2)} G^*_{P_2} G^{cc}_{C_1} G^{cc}_{C_2} R^m_{1,j})}_{CD/FFD}\\
\quad \left. - \underbrace{q^{-(2f_2+2)} S((G^*_{P_2})^2 G^{cc}_{C_2} G^{ff}_{C_{1,j}} + q^{-(f_1+1)} G^*_{P_1} G^*_{P_2} G^{cc}_{C_1} G^{cc}_{C_2} G^{ff}_{C_{1,j}})}_{CD/FFD} \right] w^m_{1,j}
\end{array} \right\}\\
&\quad + \left\{ \begin{array}{l}
\sum_{i=1}^{N} \left[ \underbrace{q^{-(l_{2,i}+1)} Q^m_{2,i}}_{CI/FFI} + \underbrace{q^{-(f_2+1)} G^*_{P_2} G^{ff}_{C_{2,i}}}_{CI/FFD} \right.\\
\quad + \underbrace{q^{-(f_2+l_{2,i}+2)} S(R^m_{2,i} - G^*_{P_2} G^{cc}_{C_2} Q^m_{2,i} - G^*_{P_1} G^*_{P_2} G^{cc}_{C_1} G^{cc}_{C_2} Q^m_{2,i})}_{CD/FFD}\\
\quad \left. - \underbrace{\begin{array}{l} S(q^{-(2f_2+2)} (G^*_{P_2})^2 G^{ff}_{C_{2,i}} G^{cc}_{C_2}\\ + q^{-(f_1+2f_2+3)} G^*_{P_1} (G^*_{P_2})^2 G^{ff}_{C_{2,i}} G^{cc}_{C_1} G^{cc}_{C_2} \end{array}}_{CD/FFD} \right] w^m_{2,i} \qquad \text{if } l_{2,i} < f_2\\
\sum_{i=1}^{N} \left[ \underbrace{q^{-(f_2+1)} G^*_{P_2} G^{ff}_{C_{2,i}}}_{CI/FFD} \right.\\
\quad + \underbrace{q^{-(f_2+l_{2,i}+2)} S(R^m_{2,i} - G^*_{P_2} G^{cc}_{C_2} Q^m_{2,i} - G^*_{P_1} G^*_{P_2} G^{cc}_{C_1} G^{cc}_{C_2} Q^m_{2,i})}_{CD/FFD}\\
\quad \left. - \underbrace{\begin{array}{l} S(q^{-(2f_2+2)} (G^*_{P_2})^2 G^{ff}_{C_{2,i}} G^{cc}_{C_2}\\ + q^{-(f_1+2f_2+3)} G^*_{P_1} (G^*_{P_2})^2 G^{ff}_{C_{2,i}} G^{cc}_{C_1} G^{cc}_{C_2} \end{array}}_{CD/FFD} \right] w^m_{2,i} \qquad \text{if } l_{2,i} \geq f_2
\end{array} \right\}
\end{aligned}
\tag{5}
$$

where $S=1/(1+G_{P_2}G_{C_2}+G_{P_1}G_{P_2}G_{C_1}G_{C_2})$. In these decomposition equations, it is obvious to see from the block diagram (Fig. 1) that $Q_1^u$ is the cascade invariant of $y_1$ because the disturbance $w_1^u$ enters directly into the output $y_1$ and there is time delay ($f_2+f_1+2$) of processes $G_{P_1}$ and $G_{P_2}$. $R_1^u$ implies cascade dependent effect of $y_1$, which makes it possible for both controllers to cause a change after $f_2+f_1+2$ time delays. E is the cascade invariant of $y_1$ because the disturbance $w_2^u$ enters directly into the output $y_1$ after the time delay ($f_1+1$) of processes $G_{P_1}$. Similar explanations can be used for the relationships between $Q_2^u$ and $R_2^u$ for $y_2$. Thus, $y_{1,CC}$ of $y_1$ and $y_{2,CC}$ of $y_2$ are decomposed into the cascade invariant (CI) and the cascade dependent (CD) term. The identity of the feedforward models ($(G_{L_{1,j}}^m)^*$ and $(G_{L_{2,i}}^m)^*$) based on the dead times $f_1+f_2+2$ and $f_2+1$ may contain the feedforward invariant ($Q_{1,j}^m$ and $Q_{2,j}^m$) and the feedforward dependent ($R_{1,j}^m$ and $R_{2,j}^m$). If $l_{1,j}$ is smaller than $f_2+f_1$, $y_{1,FF}$ of $y_1$ with respect to $w_{1,j}^m$ is decomposed into the cascade invariant/feedforward invariant (CI/FFI), the cascade invariant/feedforward dependent (CI/FFD) and the cascade dependent/feedforward dependent (CD/FFD) terms; If $l_{1,j}$ is equal to or bigger than $f_2+f_1$, $y_{1,FF}$ is decomposed into the cascade invariant/feedforward dependent (CI/FFD) and the cascade dependent/feedforward dependent (CD/FFD) terms. If $l_{2,j}$ is smaller than $f_2$, $y_{1,FF}$ of $y_1$ with respect to $w_{2,j}^m$ is decomposed into the cascade invariant/feedforward invariant (CI/FFI), the cascade invariant/feedforward dependent (CI/FFD), and the cascade dependent/feedforward dependent (CD/FFD) terms; If $l_{2,j}$ is equal to or bigger than $f_2$, $y_{1,FF}$ is decomposed into the cascade invariant/feedforward dependent (CI/FFD) and the cascade dependent/feedforward dependent (CD/FFD) terms. Similar decompositions can be also applied to $y_{2,FF}$ of $y_2$.

Even though MVC is often used as a performance benchmark, it is unrealistic for general applications. It usually leads to a large input action and it is a lack of robustness in control. Thus, a more practical and achievable performance benchmark for the specific controllers can be obtained by solving the following optimization problem:

$$(\sigma_{CC/FF}^2)_{achievable\text{-}MV}=\min_{\substack{G_{C_1}^{cc},G_{C_2}^{cc}\\ G_{C_{1,j}}^{ff},G_{C_{2,i}}^{ff}}}\sigma_{CC/FF,y_1}^2 \tag{6}$$

It is apparent that the variance of the output $y_1$ is the function of the controller parameters $G_{C_1}^{cc}$, $G_{C_2}^{cc}$, $G_{C_{1,j}}^{ff}$ and $G_{C_{2,i}}^{ff}$. Note that the benchmark bound only shows if the current performance is close to the achievable benchmark. The possible faults that downgrade the control performance are still unknown.

Based on Eqs. (4)-(5), the output variances ($\sigma_{y_1}^2$ and $\sigma_{y_2}^2$) related to the impulse response coefficients can be expressed as

$$\begin{aligned}\sigma_{y_1}^2&=\sigma_{y_1,CC}^2+\sigma_{y_1,FF}^2\\ \sigma_{y_2}^2&=\sigma_{y_2,CC}^2+\sigma_{y_2,FF}^2\end{aligned} \tag{7}$$

where

$$\begin{aligned}\sigma_{y_1,CC}^2=&S_{y_1,CI_{11}}(G_{L_1}^u)\sigma_{w_1^u}^2+S_{y_1,CD_{11}}(f_1,f_2,G_{P_1}^*,G_{P_2}^*,G_{L_1}^u,G_{C_1},G_{C_2})\sigma_{w_1^u}^2\\&+S_{y_1,CI_{12}}(f_1,G_{P_1}^*,G_{L_2}^u)\sigma_{w_2^u}^2+S_{y_1,CD_{12}}(f_1,f_2,G_{P_1}^*,G_{P_2}^*,G_{L_2}^u,G_{C_1},G_{C_2})\sigma_{w_2^u}^2\end{aligned} \tag{8}$$

$$\begin{aligned}\sigma_{y_2,CC}^2=&S_{y_2,CD_{21}}(f_1,f_2,G_{P_1}^*,G_{P_2}^*,G_{L_1}^u,G_{C_1}^{cc},G_{C_2}^{cc})\sigma_{w_1^u}^2\\&+S_{y_2,CI_{22}}(G_{L_2}^u)\sigma_{w_2^u}^2+S_{y_2,CD_{22}}(f_1,f_2,G_{P_1}^*,G_{P_2}^*,G_{L_2}^u,G_{C_1}^{cc},G_{C_2}^{cc})\sigma_{w_2^u}^2\end{aligned} \tag{9}$$

$$\begin{aligned}\sigma_{y_1,FF}^2=&\sum_{j=1}^{M}\sigma_{y_1,FF,w_{1,j}^m}^2+\sum_{i=1}^{N}\sigma_{y_1,FF,w_{2,i}^m}^2\\=&\begin{cases}\sum_{j=1}^{M}(S_{y_1,CI/FFI,j}(l_{1,j},G_{L_{1,j}}^m)\sigma_{w_{1,j}^m}^2\\ \quad+S_{y_1,CI/FFD,j}(f_1,f_2,G_{L_{1,j}}^m,G_{P_1}^*,G_{P_2}^*,G_{c_{1,j}}^{ff})\sigma_{w_{1,j}^m}^2\\ \quad+S_{y_1,CD/FFD,j}(f_1,f_2,l_{1,j},G_{L_{1,j}}^m,G_{P_1}^*,G_{P_2}^*,G_{c_{1,j}}^{ff},G_{C_1}^{cc},G_{C_2}^{cc})\sigma_{w_{1,j}^m}^2)\\ \qquad\text{if } l_{1,j}<f_1+f_2\\ \sum_{j=1}^{M}(S_{y_1,CI/FFD,j}(f_1,f_2,G_{P_1}^*,G_{P_2}^*,G_{c_{1,j}}^{ff})\sigma_{w_{1,j}^m}^2\\ \quad+S_{y_1,CD/FFD,j}(f_1,f_2,l_{1,j},G_{L_{1,j}}^m,G_{P_1}^*,G_{P_2}^*,G_{c_{1,j}}^{ff},G_{C_1}^{cc},G_{C_2}^{cc})\sigma_{w_{1,j}^m}^2)\\ \qquad\text{if } l_{1,j}\ge f_1+f_2\end{cases}\\&+\begin{cases}\sum_{i=1}^{N}(S_{y_1,CI/FFI,i}(f_1,l_{2,i},G_{P_1}^*,G_{L_{2,i}}^m)\sigma_{w_{2,i}^m}^2\\ \quad+S_{y_1,CI/FFD,i}(f_1,f_2,G_{L_{2,i}}^m,G_{P_1}^*,G_{P_2}^*,G_{c_{2,i}}^{ff})\sigma_{w_{2,i}^m}^2\\ \quad+S_{y_1,CD/FFD,i}(f_1,f_2,l_{2,i},G_{L_{2,i}}^m,G_{P_1}^*,G_{P_2}^*,G_{c_{2,i}}^{ff},G_{C_1}^{cc},G_{C_2}^{cc})\sigma_{w_{2,i}^m}^2)\\ \qquad\text{if } l_{2,j}<f_2\\ \sum_{i=1}^{N}(S_{y_1,CI/FFD,i}(f_1,f_2,G_{P_1}^*,G_{P_2}^*,G_{c_{2,i}}^{ff})\sigma_{w_{2,i}^m}^2\\ \quad+S_{y_1,CD/FFD,i}(f_1,f_2,l_{2,i},G_{L_{2,i}}^m,G_{P_1}^*,G_{P_2}^*,G_{c_{2,i}}^{ff},G_{C_1}^{cc},G_{C_2}^{cc})\sigma_{w_{2,i}^m}^2)\\ \qquad\text{if } l_{2,i}\ge f_2\end{cases}\end{aligned} \tag{10}$$

$$\begin{aligned}\sigma_{y_2,FF}^2=&\sum_{j=1}^{M}\sigma_{y_2,FF,w_{1,j}^m}^2+\sum_{i=1}^{N}\sigma_{y_2,FF,w_{2,i}^m}^2\\=&\sum_{j=1}^{M}(S_{y_2,CI/FFD,j}(f_2,G_{P_2}^*,G_{c_{1,j}}^{ff})\sigma_{w_{1,j}^m}^2\\&+S_{y_2,CD/FFD,j}(f_2,l_{1,j},G_{L_{1,j}}^m,G_{P_1}^*,G_{P_2}^*,G_{c_{1,j}}^{ff},G_{C_1}^{cc},G_{C_2}^{cc})\sigma_{w_{1,j}^m}^2)\\&+\begin{cases}\sum_{i=1}^{N}(S_{y_2,CI/FFI,i}(l_{2,i},G_{L_{2,i}}^m)\sigma_{w_{2,i}^m}^2+S_{y_2,FFD(CI),i}(f_2,G_{L_{2,i}}^m,G_{P_2}^*,G_{c_{2,i}}^{ff})\sigma_{w_{2,i}^m}^2\\ \quad+S_{y_2,CD/FFD,i}(f_2,l_{2,i},G_{L_{2,i}}^m,G_{P_1}^*,G_{P_2}^*,G_{c_{2,i}}^{ff},G_{C_1}^{cc},G_{C_2}^{cc})\sigma_{w_{2,i}^m}^2)\\ \qquad\text{if } l_{2,i}<f_2\\ \sum_{i=1}^{N}(S_{y_2,CI/FFD,i}(f_2,G_{P_2}^*,G_{c_{2,i}}^{ff})\sigma_{w_{2,i}^m}^2\\ \quad+S_{y_2,CD/FFD,i}(f_2,l_{2,i},G_{L_{2,i}}^m,G_{P_1}^*,G_{P_2}^*,G_{c_{2,i}}^{ff},G_{C_1}^{cc},G_{C_2}^{cc})\sigma_{w_{2,i}^m}^2)\\ \qquad\text{if } l_{2,i}<f_2\end{cases}\end{aligned} \tag{11}$$

and

$$s_{y_1,CI_{11}}=\sum_{h=0}^{f_1}(\alpha_{y_1,w_1^u,h})^2 \qquad s_{y_1,CD_{11}}=\sum_{h=f_1+1}^{\infty}(\alpha_{y_1,w_1^u,h})^2$$

$$s_{y_1,CI_{12}}=\sum_{h=f_1+1}^{f_1+f_2+1}(\alpha_{y_1,w_2^u,h})^2 \qquad s_{y_1,CD_{12}}=\sum_{h=f_1+f_2+2}^{\infty}(\alpha_{y_1,w_2^u,h})^2$$

$$s_{y_2,CI_{22}}=\sum_{h=0}^{f_2}(\alpha_{y_2,w_2^u,h})^2 \qquad s_{y_2,CD_{21}}=\sum_{h=f_2+1}^{\infty}(\alpha_{y_2,w_1^u,h})^2 \qquad s_{y_2,CD_{22}}=\sum_{h=f_2+1}^{\infty}(\alpha_{y_1,w_2^u,h})^2$$

$$s_{y_1,CI/FFI,j}=\sum_{h=l_{1,j}+1}^{f_1+f_2+1}(\alpha_{y_1,w_{1,j}^m,h})^2 \qquad s_{y_1,CI/FFD,j}=\sum_{h=f_1+f_2+2}^{f_1+f_2+l_{1,j}+2}(\alpha_{y_1,w_{1,j}^m,h})^2$$

$$s_{y_1,CD/FFD,j}=\sum_{h=f_1+f_2+l_{1,j}+3}^{\infty}(\alpha_{y_1,w_{1,j}^m,h})^2$$

$$s_{y_1,CI/FFI,i}=\sum_{h=f_1}^{f_1+f_2+1}(\alpha_{y_2,w_{2,i}^m,h})^2 \qquad s_{y_1,CI/FFD,i}=\sum_{h=f_1+f_2+2}^{f_1+f_2+l_{2,i}+2}(\alpha_{y_2,w_{2,i}^m,h})^2$$

$$s_{y_1,CD/FFD,i}=\sum_{h=f_1+f_2+l_{2,i}+3}^{\infty}(\alpha_{y_2,w_{2,i}^m,h})^2$$

$$s_{y_2,CI/FFD,j}=\sum_{h=f_2+1}^{f_2+l_{1,j}+1}(\alpha_{y_1,w_{1,j}^m,h})^2 \qquad s_{y_2,CD/FFD,j}=\sum_{h=f_2+l_{1,j}+2}^{\infty}(\alpha_{y_1,w_{1,j}^m,h})^2$$

$$s_{y_2,CI/FFI,i}=\sum_{h=l_{2,i}+1}^{f_2}(\alpha_{y_2,w_{2,i}^m,h})^2 \qquad s_{y_2,CI/FFD,i}=\sum_{h=f_2+1}^{f_2+l_{2,i}+2}(\alpha_{y_2,w_{2,i}^m,h})^2$$

$$s_{y_2,CD/FFD,i}=\sum_{h=f_2+l_{2,i}+2}^{\infty}(\alpha_{y_2,w_{2,i}^m,h})^2$$

where $\{\alpha_{y_s,w_x^u,h}\}$ and $\{\alpha_{y_s,w_{x,j}^m,h}\}$, s=1, 2; x=1, 2 are the impulse response coefficients from $y_1$ and $y_2$. Here the unmeasured disturbances $w_1^u$ and $w_2^u$ are independent, and they are normal disturbance random variables with the same mean values of zeros; however, their variance values are different. For simplifying the above expression and easily computing the impulse response coefficients from $y_1$ and $\sigma_{w^u}^2=\sigma_{w_1^u}^2/a^2=\sigma_{w_2^u}^2/b^2$, are defined, where a and b are constant ratios for extracting a common unmeasured disturbance ($w^u$) for and $w_1^u$ and $w_2^u$. The above equations can be written as

$$\sigma_{y_1,CC}^2=s_{y_1,CI}(G_{L_1}^u)\,\sigma_{w^u}^2+s_{y_1,CD}(f_1,f_2,G_{P_1}^*,G_{P_2}^*,G_{L_1}^u,G_{L_2}^u)\sigma_{w^u}^2$$
$$\sigma_{y_2,CC}^2=s_{y_2,CI}(G_{L_2}^u)\,\sigma_{w^u}^2+s_{y_2,CD}(f_1,f_2,G_{P_1}^*,G_{P_2}^*,G_{L_1}^u,G_{L_2}^u)\sigma_{w^u}^2 \qquad (13)$$

where

$$s_{y_1,CI}=\sum_{h=0}^{f_1}(a\alpha_{y_1,w_1^u,h})^2 \quad s_{y_1,CD}=\sum_{h=f_1+1}^{\infty}[(a\alpha_{y_1,w_1^u,h})^2+(b\alpha_{y_1,w_2^u,h})^2]$$
$$s_{y_2,CI}=\sum_{h=0}^{f_2}(b\alpha_{y_2,w_2^u,h})^2 \quad s_{y_2,CD}=\sum_{h=f_2+1}^{\infty}[(a\alpha_{y_2,w_1^u,h})^2+(b\alpha_{y_2,w_2^u,h})^2] \qquad (14)$$

In Eq. (13), the output variance $\sigma_{y_1,CC}^2$ can be classified into the variances from CI ($s_{y_1,CI}$) and from CD ($s_{y_1,CD}$). $s_{y_1,CI}$ is the sum of the first ($f_1$+1) square impulse response coefficients of the effect $w_1$ on $y_1$. Thus, it is the function of $G_{L_1}^u$ only. $s_{y_1,CD}$ is the sum of the square impulse response coefficients of the rest terms from $f_1$+1, including $CD_{11}$, $CD_{12}$ and part of $CI_{12}$. Similar explanations are used for $s_{y_2,CI}$ and $s_{y_2,CD}$.

## FAULT DETECTION AND DIAGNOSIS OF A FEEDFORWARD/CASCADE CONTROL SYSTEM

Assume the operating controllers ($G_{C_1,j}^{ff}$, $G_{C_2,i}^{ff}$, $G_{C_1}^{cc}$ and $G_{C_2}^{cc}$) with the achievable performance are given. The faults from these operating controllers can be checked first before starting diagnosis. The possible fault sources would come from the other elements ($f_1$, $f_2$, $l_{1,j}$, $l_{2,i}$, $G_{P_1}$, $G_{P_2}$, $G_{L_1}^u$, $G_{L_2}^u$, $G_{L_1,j}^m$ and $G_{L_2,i}^m$). In the terms of the output variances of the feedforward and the cascade loops (Eqs. (10)-(11) and (13)), the dead times ($f_1$, $f_2$, $l_{1,j}$ and $l_{2,i}$) are used to divide the variance into CI, CD, CI/FFI, CI/FFD and CD/FFD. The dead times for the current operating data should be estimated first and checked if they are changed. Here the correlation analysis method is adopted [12]. This time delay can be estimated based on the maximum value of the cross correlation between the process input and the output of the closed loop data [13]. Other techniques can also help determining the process dead time from the closed-loop data [14].

### 1. Cascade Control Loop

Because the operating controllers and the dead times have been checked before, now the possible fault causes ($G_{P_1}^*$, $G_{P_2}^*$, $G_{L_1}^u$ and $G_{L_2}^u$) can be found by examining corresponding sub-terms ($S_{y_1,CI}$, $S_{y_1,CD}$, $S_{y_2,CI}$ and $S_{y_2,CD}$) of $\sigma_{y_1,CC}^2$ and $\sigma_{y_2,CC}^2$ for the current and the achieved conditions.

$$(CI)_0^1:\ S_{y_1,(CI)_0}^*=S_{y_1,(CI)_0}^c \quad (CD)_0^1:\ S_{y_1,(CD)_0}^*=S_{y_1,(CD)_0}^c$$
$$(CI)_0^2:\ S_{y_2,(CI)_0}^*=S_{y_2,(CI)_0}^c \quad (CD)_0^2:\ S_{y_2,(CD)_0}^*=S_{y_2,(CD)_0}^c \qquad (15)$$

where S with the superscripts * and c, represents the achieved and current conditions, respectively. Because the disturbances are driven by white noise sequences, the ratios $S_{y_1,(CI)_0}^c/S_{y_1,(CI)_0}^*$, $s_{y_1,(CD)_0}^c/s_{y_1,(CD)_0}^*$,

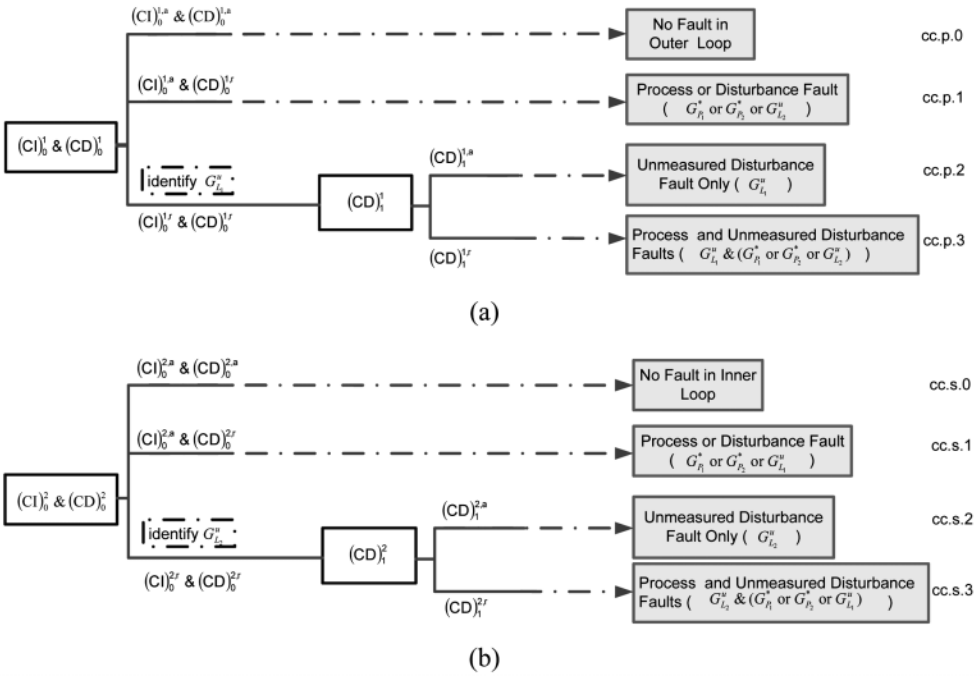


**Fig. 2. Fault detection and diagnosis trees for (a) the primary control output and (b) the second control output.**

**Table 1. The diagnosis rules of the cascade control loops by merging the primary and the secondary diagnosis trees**

| Diagnosis result / Fault symptom of the primary loop / Fault symptom of the secondary loop | cc.p.1 | cc.p.2 | cc.p.3 |
|---|---|---|---|
| cc.s.1 | $G_{P_1}$ or $G_{P_2}$ | $G^u_{L_1}$ | $G^u_{L_1}$ & ($G_{P_1}$ or $G_{P_2}$) |
| cc.s.2 | $G^u_{L_2}$ | — | — |
| cc.s.3 | $G^u_{L_2}$ & ($G_{P_1}$ or $G_{P_2}$) | — | $G^u_{L_1}$ & $G^u_{L_2}$ or ($G_{P_1}$ or $G_{P_2}$) |

$S^c_{y_2,(CI)_0}/S^*_{y_2,(CI)_0}$ and $s^c_{y_2,(CD)_0}/s^*_{y_2,(CD)_0}$ follow a distribution called the F distribution [15]. Based on the quantified variation of both terms, the appropriate threshold for the F statistics can be determined to identify what are the fault conditions in the current operation.

Two diagnosis trees for the primary and the secondary control loops are shown in Fig. 2(a) and (b), respectively. Each tree will branch to three child nodes ($(CI)^{i,a}_0$ & $(CD)^{i,a}_0$, $(CI)^{i,a}_0$ & $(CD)^{i,r}_0$, and $(CI)^{i,r}_0$ & $(CD)^{i,r}_0$, where the superscripts "a" and "r" represent the accepted and rejected outcomes, respectively, and the superscript "i" represents the primary (i=1) or the secondary output (i=2), respectively.

(a) $(CI)^{i,a}_0$ & $(CD)^{i,a}_0$.

It indicates no fault in the feedback loop (cc.p.0 in Fig. 2(a) and cc.s.0 in Fig. 2(b)).

(b) $(CI)^{i,a}_0$ & $(CD)^{i,r}_0$

$S_{y_i,CI}$ is the function of the unmeasured disturbance model ($G^u_{L_i}$). $(CI)^{i,a}_0$ shows that $G_{Li}$ has no fault. Thus, $(CD)^{i,r}_0$ indicates that the possible faults are from $G^*_{P_1}$, $G^*_{P_2}$ or $G^u_{L_j}$, j≠i error (cc.p.1 in Fig. 2(a) and cc.s.1 in Fig. 2(b)).

(c) $(CI)^{i,r}_0$ & $(CD)^{i,r}_0$

$(CI)^{i,r}_0$ & $(CD)^{i,r}_0$ indicate $G^u_{L_i}$ error must exist. In order to re-construct the unmeasured disturbance model, the disturbance model ($G^u_{L_i}$) is identified based on the first $f_i$+1 closed loop impulse response coefficients obtained from the time-series modeling of the current output operating data. The approximate stochastic disturbance model realization (ASDR) [16] is adopted here to identify the disturbance model that can only be identified by using routine output data. The method is good for the accurate disturbance model when there are three or more dead times. Other identifications of the disturbance model can also be applied [2,17]. After $G^u_{L_i}$ is substituted into $(CD)^i$, other faults can be further examined by using the hypothesis test ($(CD)^i_1$),

$$(CD)^i_1: S^c_{y_i,(CD)_1} = S^*_{y_i,(CD)_1} \quad (16)$$

Thus, the above node can be further branched to two child nodes:

(i) If $(CD)^i_1$ is accepted, the only fault is $G^u_{L_i}$ (cc.p.2 in Fig. 2(a) and cc.s.2 in Fig. 2(b)).

(ii) If $(CD)^i_1$ is rejected, it represents faults from $G^u_{L_i}$ as well as from any one or all of $G^*_{P_1}$, $G^*_{P_2}$ and $G^u_{L_j}$, j≠i (cc.p.3 in Fig. 2(a) and cc.s.3 in Fig. 2(b)).

Note that the condition ($(CI)^{i,r}_0$ & $(CD)^{i,a}_0$) does not exist. Whenever any $(CI)^i_0$ fault occurs, the $(CD)^i_0$ term must be unacceptable because the $(CI)^i_0$ fault coming from the change of the disturbance model will also affect the impulse coefficients of the $(CD)^i_0$ term.

In order to identify the possible fault from the CC loops, simply combine the rules of the two individual diagnosis trees produced in the above steps into a new set of rules shown in Table 1. The columns and the rows labeled (cc.p.i and cc.s.j, i, j=1, 2, 3) represent three fault conditions of each individual control loop. There are nine possible rules in the combined rule set, but the normal condition rule of each control output is not included. Due to the interaction of the cascade control system, the control output must be accepted when the other control output is accepted. In Table 1, the interaction of any two individual rules may be put into a specific fault condition. For instance, when the symptom of the primary loop is cs.p.1 ($(CI)^{1,a}_0$ & $(CD)^{1,r}_0$) and the symptom of the secondary one is cc.s.1 ($(CI)^{2,a}_0$ & $(CD)^{2,r}_0$), the former indicates that the fault $G^u_{L_1}$ does not exist and the latter shows that the fault $G^u_{L_2}$ also does not happen. Thus, the faults in the current system would come from the process models ($G^*_{P_1}$ or $G^*_{P_2}$). However, some combination may lead to the conflict condition. For example, when the symptom of the primary loop is cs.p.2 ($(CD)^{1,a}_1$) and the symptom of the secondary one is cs.s.3 ($(CD)^{2,r}_1$), the former indicates that the only fault is $G^u_{L_1}$, but the latter shows that the other possible faults ($G^u_{L_1}$ or $G^*_{P_1}$ or $G^*_{P_2}$) must occur and the fault $G^u_{L_2}$ must exist. Thus, the conflict condition should be removed, which is marked in bold line in Table 1. Similar explanations can be used for the other symptom pairs in the box of Table 1, except for the condition when the symptoms of the control loop are cc.p.3 ($(CD)^{1,r}_1$) and cc.s.3 ($(CD)^{2,r}_1$). In this condition, both $G^u_{L_1}$ and $G^u_{L_2}$ have errors, but it does not show whether $G^*_{P_1}$ or $G^*_{P_2}$ has the model error. Thus, the disturbance models ($G^u_{L_1}$ and $G^u_{L_2}$) should be updated to isolate these faults, and then the diagnostic tree of each loop is applied again. If the process models are mismatched, the final faults must be ($G^*_{P_1}$ or $G^*_{P_2}$) as well as ($G^u_{L_1}$ and $G^u_{L_2}$); otherwise, the only faults must be ($G^u_{L_1}$ and $G^u_{L_2}$).

**2. Feedforward Control Loop**

In Fig. 1, there are two different types of the measured disturbances ($G^m_{L_1,j}$, j=1, …, M and $G^m_{L_2,i}$, i=1, …, N) in the control system. $G^m_{L_1,j}$ and $G^m_{L_2,i}$ directly enter the primary and the second outputs, respectively. From the variances of the control outputs ($\sigma^2_{y_1,FF,w^m_{1,j}}$ and $\sigma^2_{y_2,FF,w^m_{2,j}}$), the terms of $S_{y_1,CI/FF1,j}$ and $S_{y_2,CI/FF1,i}$ are the only functions of the measured disturbance models, $G^m_{L_1,j}$ and $G^m_{L_2,i}$, respectively. As for the diagnosis trees of the feedforward loops of $\sigma^2_{y_1,FF,w^m_{1,j}}$ and $\sigma^2_{y_2,FF,w^m_{2,j}}$ (Fig. 3), two conditions are separated based on the difference of the dead times between the processes and the measured disturbances ($l_{1,j}<f_1+f_2$ and $l_{1,j}\geq f_1+f_2$ for $\sigma^2_{y_1,FF,w^m_{1,j}}$; $l_{2,i}<f_2$ and $l_{2,i}\geq f_2$ for $\sigma^2_{y_2,FF,w^m_{2,i}}$).

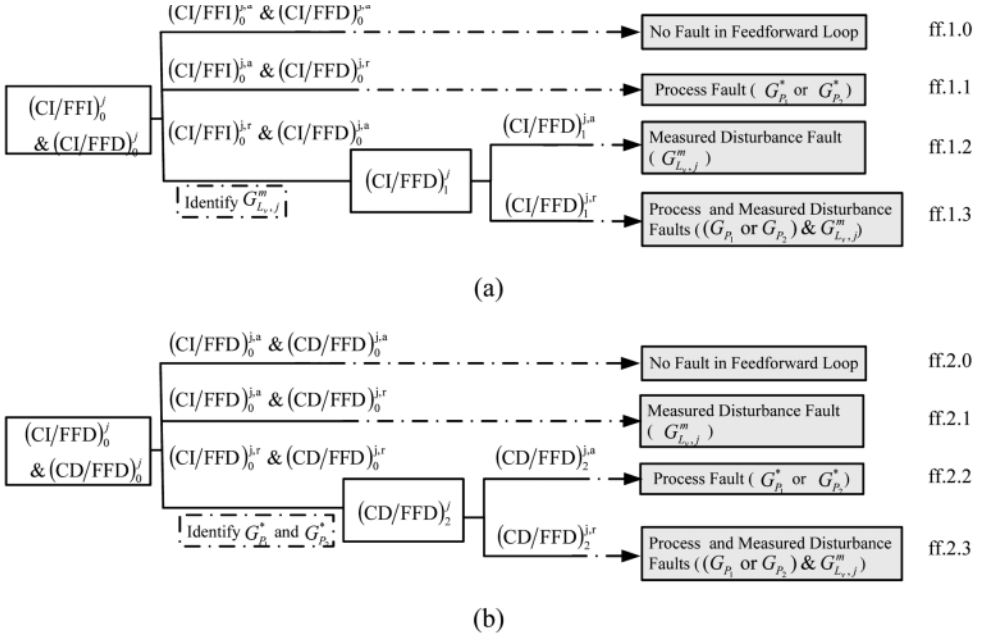


**Fig. 3. Fault detection and diagnosis tree for the feedforward control loop: (a) $l_{1,j}<f_1+f_2$ or $l_{2,i}<f_2$; (b) $l_{1,j}\geq f_1+f_2$ or $l_{2,i}\geq f_2$.**

**Condition 1:** $l_{1,j}<f_1+f_2$ (or $l_{2,j}<f_2$) j=1, 2, …

$$\sigma^2_{y_v,FF,w^m_{v,j}} = S_{y_v,CI/FFI,j}(G^m_{L_v,j})\,\sigma^2_{w^m_{v,j}} + S_{y_v,CI/FFD,j}(G^m_{L_v,j}, G^*_{P_1}, G^*_{P_2})\,\sigma^2_{w^m_{v,j}} + S_{y_v,CD/FFD,j}(G^m_{L_v,j}, G^*_{P_1}, G^*_{P_2})\,\sigma^2_{w^m_{v,j}} \quad v=1,2 \tag{17}$$

where $S_{y_v,CI/FFD,j}$ and $S_{y_v,CD/FFD,j}$ are the functions of the same elements. Thus, only the hypothesis testing of $S_{y_v,CI/FFI,j}$ and $S_{y_v,CI/FFD,j}$ based on the achievable minimum and the current variances used here is evaluated.

$$(CI/FFI)_0^j\text{: } S^c_{y_v,(CI/FFI)_0^j} = S^*_{y_v,(CI/FFI)_0^j}$$
$$(CI/FFD)_0^j\text{: } S^c_{y_v,(CI/FFD)_0^j} = S^*_{y_v,(CI/FFD)_0^j} \tag{18}$$

With the two null hypothesis testing, three possible outcomes would happen:

(a) $(CI/FFI)_0^{j,a}$ & $(CI/FFD)_0^{j,a}$:

It shows there is no fault in the feedforward loop (ff.1.0 in Fig. 3(a)).

(b) $(CI/FFI)_0^{j,a}$ & $(CI/FFD)_0^{j,r}$:

The acceptance of $(CI/FFI)_0^j$ indicates that $G^m_{L_v,j}$ is no fault. This implies that the rejection of $(CI/FFD)_0^j$ comes from the fault of $G^*_{P_1}$ or $G^*_{P_2}$ (ff.1.1 in Fig. 3(a)).

(c) $(CI/FFI)_0^{j,r}$ & $(CI/FFD)_0^{j,r}$:

$(CI/FFI)_0^j$ exceeds the critical value of the hypothesis testing. $(CI/FFI)_0^j$ cannot also be accepted. One of the possible faults must be from the disturbance model ($G^m_{L_v,j}$). The measured disturbance model should be re-estimated. With the estimated $G^m_{L_v,j}$, the new CI/FFD of the achievable is updated. The node based on the new hypothesis testing of $(CI/FFD)_1^j$ is further branched into two child nodes:

(i) If $(CI/FFD)_1^j$ is accepted, the only fault is $G^m_{L_v,j}$ (ff.1.2 in Fig. 3(a))

(ii) If $(CI/FFD)_1^j$ is still rejected, it represents faults from $G^m_{L_v,j}$ and ($G^*_{P_1}$ or $G^*_{P_2}$) (ff.1.3 in Fig. 3(a)).

**Condition 2:** $l_{1,j}\geq f_1+f_2$ (or $l_{2,j}\geq f_2$) j=1, 2, …

$$\sigma^2_{y_v,FF,w^m_{v,j}} = S_{y_v,CI/FFD,j}(G^*_{P_1}, G^*_{P_2})\,\sigma^2_{w^m_{v,j}} + S_{y_v,CD/FFD,j}(G^m_{L_v,j}, G^*_{P_1}, G^*_{P_2})\,\sigma^2_{w^m_{v,j}} \quad v=1,2 \tag{19}$$

Like Condition 1, the evaluation of the hypothesis testing of $S_{y_v,CI/FFD,j}$ and $S_{y_v,CD/FFD,j}$ based on the achievable minimum and the current variances is

$$(CI/FFD)_0^j\text{: } S^c_{y_v,(CI/FFD)_0^j} = S^*_{y_v,(CI/FFD)_0^j}$$
$$(CD/FFD)_0^j\text{: } S^c_{y_v,(CD/FFD)_0^j} = S^*_{y_v,(CD/FFD)_0^j} \tag{20}$$

Also, they have three possible outcomes:

(a) $(CI/FFD)_0^{j,a}$ & $(CD/FFD)_0^{j,a}$:

It represents there is no fault in the feedforward loop (ff.2.0 in Fig. 3(b)).

(b) $(CI/FFD)_0^{j,a}$ & $(CD/FFD)_0^{j,r}$:

The acceptance of $(CI/FFD)_0^j$ explains $G^*_{P_1}$ and $G^*_{P_2}$ are correct. This implies that the rejection of $(CD/FFD)_0^j$ comes from the fault of $G^m_{L_v,j}$ (ff.2.1 in Fig. 3(b)).

(c) $(CI/FFD)_0^{j,r}$ & $(CD/FFD)_0^{j,r}$:

The $(CI/FFD)_0^j$ exceeds the critical value of the hypothesis testing and $(CD/FFD)_0^j$ cannot also be accepted. One of the possible faults from $G^*_{P_1}$ or $G^*_{P_2}$ must exist. In order to confirm if the only fault is $G^*_{P_1}$ or $G^*_{P_2}$, the process model should be re-estimated. The conventional closed-loop model identification is applied here directly to obtain the new estimated process model. Without any external input to change the current operating process, the process models are still

consistently estimated because the excitation information of the current operating data is sufficient at poor performance.

Then the new of the achievable value is updated.

$$(\mathrm{CD/FFD})_2^j:\ \mathrm{S}^{c}_{y_i,(CD/FFD)_2^j}=\mathrm{S}^{*}_{y_i,(CD/FFD)_2^j} \tag{21}$$

The node based on the new hypothesis testing of $(\mathrm{CD/FFD})_2^j$ is further branched into two child nodes:

(iii) If $(\mathrm{CD/FFD})_2^j$ is accepted, the only fault is $G^*_{P_1}$ or $G^*_{P_2}$ (fb.2.2 in Fig. 3(b))

(iv) If $(\mathrm{CD/FFD})_2^j$ is still rejected, it represents faults from $G^m_{L_v,j}$ and from any one or all of $G^*_{P_1}$ and $G^*_{P_2}$ (fb.2.3 in Fig. 3(b)).

To sum up, a stepwise diagnosis procedure is plotted in Fig. 4. First, the fault detection and diagnosis approaches are initiated if and only if the current output variances ($\sigma^2_{y_1^c}$ and $\sigma^2_{y_2^c}$) significantly deviate from the initial benchmark ($\sigma^2_{y_1^*}$ and $\sigma^2_{y_2^*}$). The cascade control loops and then the feedforward control loops are detected separately. In the cascade control loops of Fig. 4, with the variance terms of the current closed-loop operation ($\mathrm{S}^c_{y_1,CI}$, $\mathrm{S}^c_{y_1,CD}$, $\mathrm{S}^c_{y_2,CI}$, $\mathrm{S}^c_{y_2,CD}$) and the benchmark condition ($\mathrm{S}^*_{y_1,CI}$, $\mathrm{S}^*_{y_1,CD}$, $\mathrm{S}^*_{y_2,CI}$, $\mathrm{S}^*_{y_2,CD}$), the fault detection diagnosis trees (Fig. 2) of the primary loop and the secondary loop are used to check if the faults occur. Under the hypothesis test, as long as the value of the test statistics exceeds the threshold value, the effect of the just-identified fault is fixed. Then the benchmark models are successively replaced whenever any fault is identified. As for the feedforward control in the outer loop, the diagnosis tree (Fig. 3) is applied based on the variances of the current closed-loop data ($\mathrm{S}^c_{y_1,CI/FFI,j}$, $\mathrm{S}^c_{y_1,CI/FFD,j}$ and $\mathrm{S}^c_{y_1,CD/FFD,j}$) and computation with the benchmark condition ($\mathrm{S}^*_{y_1,CI/FFI,j}$, $\mathrm{S}^*_{y_1,CI/FFD,j}$ and $\mathrm{S}^*_{y_1,CD/FFD,j}$). Likewise, based on the variances of the current closed-loop data ($\mathrm{S}^c_{y_2,CI/FFI,i}$, $\mathrm{S}^c_{y_2,CI/FFD,i}$ and $\mathrm{S}^c_{y_2,CD/FFD,i}$) and computation with the benchmark condition ($\mathrm{S}^*_{y_2,CI/FFI,i}$, $\mathrm{S}^*_{y_2,CI/FFD,i}$ and $\mathrm{S}^*_{y_2,CD/FFD,i}$), the diagnosis tree (Fig. 3) of the feedforward control in the inner loop is conducted. The stepwise diagnosis procedure is repeated until all possible faults in the cascade and the feedforward loops are detected. Note that the only possible faults from the measured disturbance models in the feedforward loop should be detected when the cascade control loops are tested first, because the other fault elements have been explored and identified in the cascade control loops.

## ILLUSTRATION EXAMPLE

The process output transfer functions related to the second controller output ($u_2(k)$), two unmeasurable disturbances ($w_1^u(k)$ and $w_2^u(k)$) and two measurable disturbance ($w_1^m(k)$ and $w_2^m(k)$) are

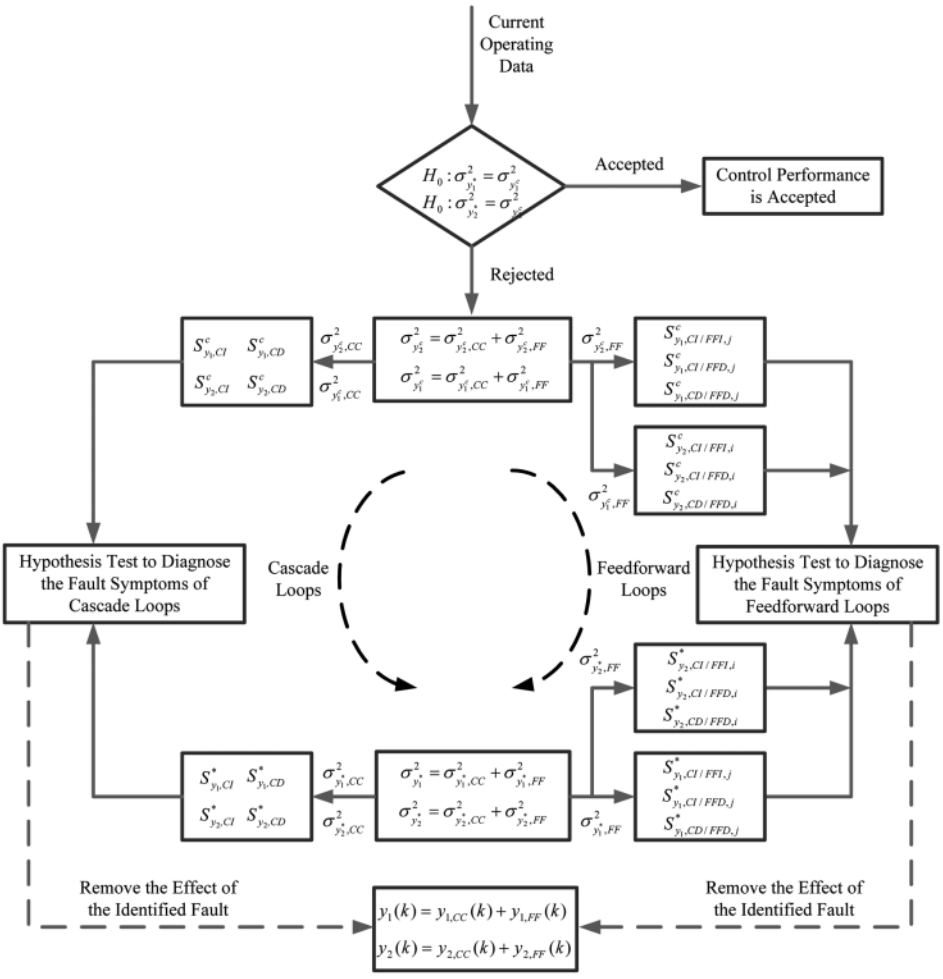


**Fig. 4. The flowchart of the stepwise diagnosis procedure.**

depicted as

$$y_1 = \frac{1}{1-0.2z^{-1}}y_2(k-9) + \frac{1}{1-0.7z^{-1}}w_1^u + \frac{z^{-5}}{1-0.7z^{-1}}w_1^m$$
$$y_2 = \frac{1}{1-0.5z^{-1}}u_2(k-9) + \frac{1}{1-0.1z^{-1}}w_2^u + \frac{z^{-5}}{1-0.2z^{-1}}w_2^m \quad (22)$$

The achievable minimum variance of this system is 2.1474 and two controllers are a PID controller for the outer loop and a PI controller for the inner loop. The achievable minimum variance of this system can be separated into CI, CD, FBI/FFI, FBI/FFD and FBD/FFD,

$$S^*_{y_1,(CI)_0^1} = 1.9600 \qquad S^*_{y_1,(CD)_0^1} = 7.6666\times10^{-4}$$
$$S^*_{y_2,(CI)_0^2} = 1.0101 \qquad S^*_{y_2,(CD)_0^2} = 5.8409\times10^{-8}$$
$$S^*_{y_1,(CI/FFI)_0^1} = 1.9607 \qquad S^*_{y_1,(CI/FFD)_0^1} = 8.5980\times10^{-5}$$
$$S^*_{y_2,(CI/FFD)_0^2} = 1.0417 \qquad S^*_{y_2,(CI/FFD)_0^2} = 0.1040 \quad (23)$$

Assume that the system model is degraded:

$$y_1 = \frac{1}{1-0.6z^{-1}}y_2(k-11) + \frac{1}{1-0.7z^{-1}}w_1^u + \frac{z^{-5}}{1-0.9z^{-1}}w_1^m$$
$$y_2 = \frac{1}{1-0.7z^{-1}}u_2(k-9) + \frac{1}{1-0.5z^{-1}}w_2^u + \frac{z^{-11}}{1-0.5z^{-1}}w_2^m \quad (24)$$

The multiple faults we consider in this case are the changes of both process models, the change of the 2*nd* unmeasured disturbance model, the change of the delay of the 2*nd* measured disturbance model, and the changes of both measured disturbance models. The control parameters are still based on the original achievable design values. The simulated closed loop output is plotted in Fig. 5. The controlled output variance of this fault condition (4.5125) is far from that of the original benchmark condition. Although the output variances of the normal and the fault conditions are significantly different, it is difficult to isolate the root fault only from the output response plot. The proposed diagnostic procedures are adopted to examine the capability.

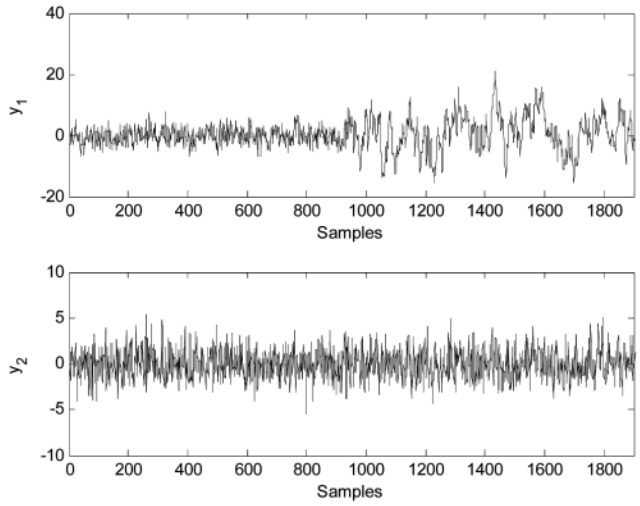


**Fig. 5. Output responses under the normal condition (before the 1000*th* sampling point) and the faulty condition (after the 1000*th* sampling point).**

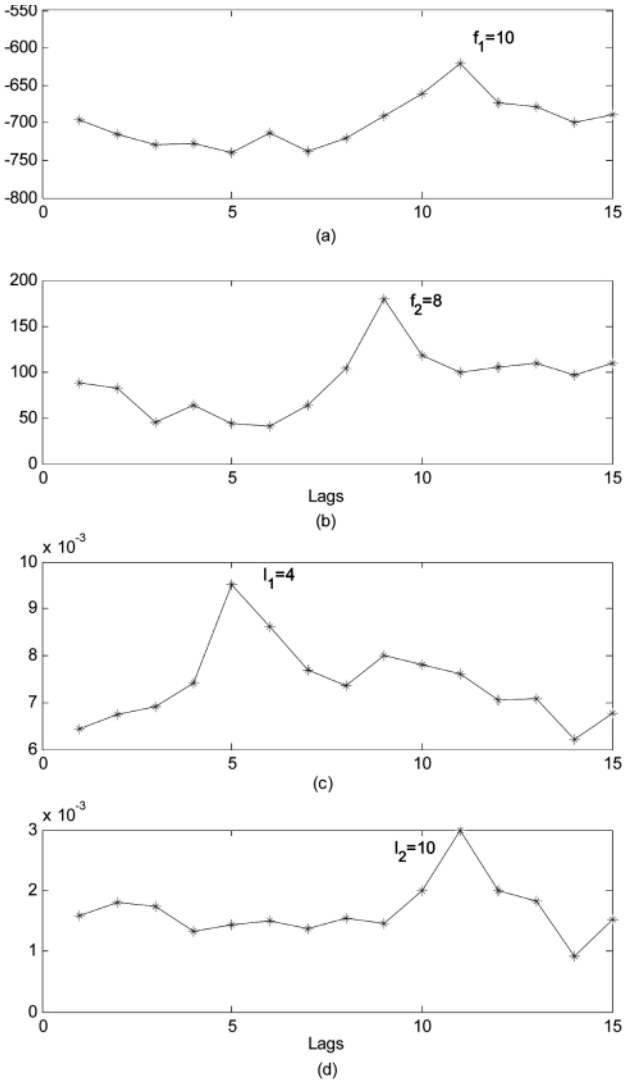


**Fig. 6. Process delay estimations: (a) the primary delay, (b) the secondary delay, (c) the first measured disturbance delay, and (d) the second measured disturbance delay.**

## 1. Diagnosis of the Cascade Loops

To isolate the possible faults from the cascade loop, the current process dead times are checked by cross-correlation analysis for the input and the output data collected from the current closed loop operating data. From Fig. 6, it is obvious that the delays of both process models are the same as their original values. Based on the guides of the diagnosis tree (Fig. 2), the hypothesis test of $(CI)_0^1$ & $(CD)_0^1$ and $(CI)_0^2$ & $(CD)_0^2$ is conducted,

$$F_{0.975} = 0.8834 < (CI)_0^1 = \frac{1.9600}{1.9600} = 1 < F_{0.025} = 1.1319$$
$$(CD)_0^1 = \frac{0.0014}{7.6666\times10^{-4}} = 1.8268 > F_{0.025} = 1.1319$$
$$(CI)_0^2 = \frac{1.3333}{1.0101} = 1.3120 > F_{0.025} = 1.1319$$
$$(CD)_0^2 = \frac{7.7331\times10^{-8}}{6.4912\times10^{-9}} = 1.3240 > F_{0.025} = 1.1319 \quad (25)$$

At the 0.05 level of significance, the hypothesis test of $y_1$ is $(CI)_0^{1,a}$ &

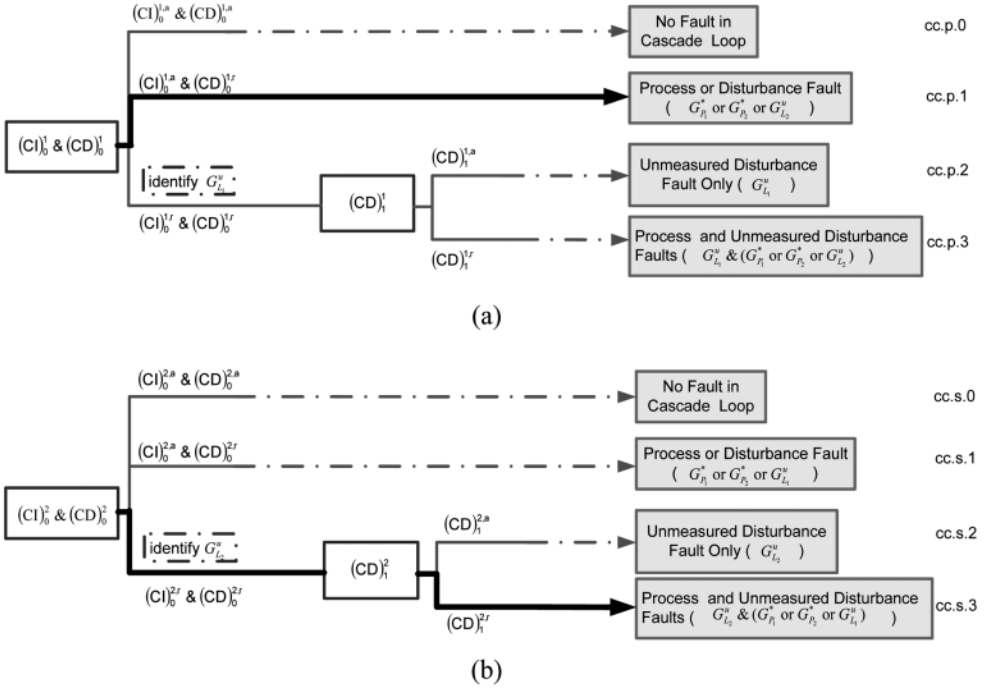


**Fig. 7. Fault detection diagnosis trees of (a) the primary loop and (b) the secondary loop whose bold line indicates the fault condition.**

$(CD)_0^{1,r}$ and that of $y_2$ is $(CI)_0^{2,r}$ & $(CD)_0^{2,r}$. According to the symptom of $(CI)_0^{1,a}$ & $(CD)_0^{1,r}$, $(CI)_0^{1,a}$ indicates there is no fault in $G_{L_1}^u$, and $(CD)_0^{1,r}$ indicates the faults are from $G_{P_1}^*$, $G_{P_2}^*$ or $G_{L_2}^u$. The fault location of the outer loop in the diagnosis tree is shown in Fig. 7(a). As for the symptom of $(CI)_0^{2,r}$ & $(CD)_0^{2,r}$, the fault comes from the unmeasured disturbance ($G_{L_2}^u$) of the inner loop. To isolate the fault, the disturbance model is re-identified by ASDR from the current operating data,

$$G_{L_2}^u = \frac{z^{-1}}{(1-0.1z^{-1})(1-0.2z^{-1})(1+0.1z^{-1})(1+0.1z^{-1})} \tag{26}$$

After the estimated disturbance model is updated, the $(CD)_1^2$ statistics is used to detect if there are other possible faults ($G_{P_1}^*$, $G_{P_2}^*$ or $G_{L_1}^u$). At the 0.05 level of significance, the null hypothesis of $(CD)_1^2$ cannot be accepted ($(CD)_1^{2,r}$),

$$(CD)_1^2 = \frac{1.1403\times10^{-5}}{4.5112\times10^{-5}} = 2.5277 > F_{0.025} = 1.1319 \tag{27}$$

Therefore, based on the output response of $y_2$, it indicates the faults come not only from $G_{L_2}^u$ but also from $G_{P_1}^*$, $G_{P_2}^*$ or $G_{L_1}^u$. The fault location of the inner loop in the diagnosis tree is shown in Fig. 7(b). Table 2 that shows the interaction of these two trees can sufficiently indicate that there are faults from $G_{L_2}^u$ as well as from any one or all of $G_{P_1}^*$ and $G_{P_2}^*$.

**2. Diagnosis of the Feedforward Loops**

First, the dead times in these two measured disturbance processes are examined. Fig. 6 shows the dead time of the first measured disturbance process is the same as its original value ($l_1$=4), and the dead time of the second measured disturbance process increases to $l_2$=10. Thus, the feedforward terms of the new achievable minimum variance benchmark are:

$$S^*_{y_1,(CI/FFD)_0^1} = 1.9607 \qquad S^*_{y_1,(CI/FFD)_0^1} = 1.0586\times10^{-4}$$
$$S^*_{y_2,(CI/FFD)_0^2} = 1.0417 \qquad S^*_{y_2,(CD/FFD)_0^2} = 2.5056\times10^{-6} \tag{28}$$

because the delay time of the 1st measured disturbance model ($l_1$+1 =5) is less than the process dead time ($f_1+f_2+2$=20), and the delay time of the 2nd measured disturbance model ($l_2$+1=11) is bigger than the process dead time ($f_2$+1=9).

(i) Feedforward loop 1:

Since $l_1<f_1+f_2+1$, based on the diagnosis tree (Fig. 3(a)), the hy-

**Table 2. Diagnostic results from the cascade loops**

| Diagnosis result / Fault symptom of the primary loop / Fault symptom of the secondary loop | cc.p.1 | cc.p.2 | cc.p.3 |
|---|---|---|---|
| cc.s.1 | $G_{P_1}$ or $G_{P_2}$ | $G_{L_1}^u$ | $G_{L_1}^u$ & ($G_{P_1}$ or $G_{P_2}$) |
| cc.s.2 | $G_{L_2}^u$ | — | — |
| cc.s.3 | $G_{L_2}^u$ & ($G_{P_1}$ or $G_{P_2}$) | — | $G_{L_1}^u$ & $G_{L_2}^u$ or ($G_{P_1}$ or $G_{P_2}$) |

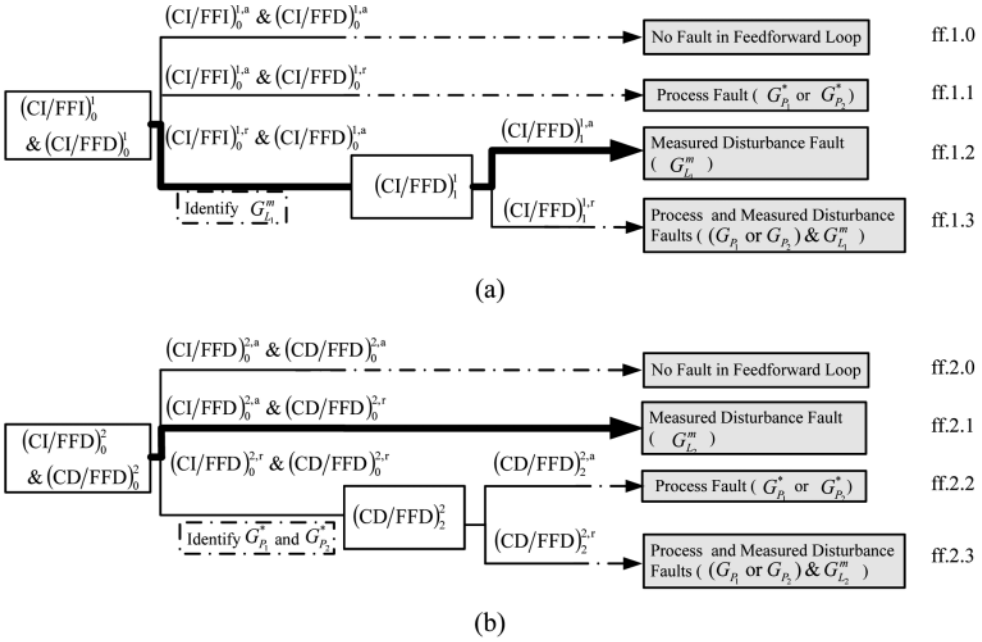


**Fig. 8. Fault detection diagnosis trees of (a) the feedforward loop 1 and (b) the feedforward loop 2 whose bold line indicates the fault condition.**

pothesis tests of $(CI/FFI)_0^1$ & $(CI/FFD)_0^1$ statistics

$$(CI/FFI)_0^1 = \frac{5.0400}{1.9607} = 2.5705 > F_{0.025} = 1.1319$$

$$(CI/FFD)_0^1 = \frac{0.1988}{1.0586\times 10^{-4}} = 1877 > F_{0.025} = 1.1319 \quad (29)$$

implies that only the 1st measured disturbance model ($G_{L_1}^m$) error exists, because the process model errors have been detected in the cascade loop. The diagnostic tree of the 1st feedforward loop is plotted in Fig. 8(a).

(ii) Feedforward loop 2:

Since $l_2 > f_2$, the diagnosis tree based on Fig. 3(b) is guided. The hypotheses test of $(CI/FFD)_0^2$ and $(CI/FFD)_0^2$ statistics,

$$F_{0.975} = 0.8834 < (CI/FFI)_0^2 = \frac{1.0989}{1.0417} = 1.0549 < F_{0.025} = 1.1319$$

$$(CI/FFD)_0^2 = \frac{0.1988}{1.0586\times 10^{-4}} = 1877 > F_{0.025} = 1.1319 \quad (30)$$

indicates that the possible fault in the 2nd feedforward loop is $G_{L_2}^m$ error. The diagnostic path is also plotted in Fig. 8(b).

From the above procedures, the identified faults are $l_2$, $G_{L_2}^u$, $G_{L_1}^m$, $G_{L_2}^m$ and ($G_{P_1}^*$ or $G_{P_2}^*$), all of which deteriorate the control performance. The last stage, but not the least one, recovers the control performance after correcting the fault sources. After these fault elements are corrected, the new achievable benchmark is 3.5248. The performance bound will be used as the new benchmark to keep monitoring and diagnosing the next coming operation cascade/feedforward system.

## CONCLUSION

A systematic approach for the needs of fault diagnosis of the FF/CC control system has been shown, including the function of controller performance assessment, the detection and diagnosis related to both FF and CC loops. The approach consists of three major stages:

1. Performance assessment: to detect the current operation of the control system if it is accepted.
2. Variance decomposition: to partition the variance information into a set of feature terms. The terms contain the key elements of the controlled system.
3. Features diagnosis: to screen out the fault element of the controlled system.

At the stage of performance assessment, by comparing the difference between the minimum variance of the controlled output and the current variance of the controlled output, the performance of the current controlled system is evaluated. The benchmark performance can just be viewed as grey indicators because these index values only imply how poor the performance of the current control loop is, not finding out and removing the fault causes associated with the performance degradation. At the variance decomposition stage, due to different impulses (of Eqs. (4)-(5)) effect on the variance of the controlled output being exhibited in different faults, the control output variances is decomposed into the cascade loop variances and the combination of cascade and feedback loop variances from the available historical data information. These decomposed variances can construct two separate sets of the diagnostic reasoning trees to analyze and find out different types of faults that can affect the achievable performance working condition. At the feature diagnosis stage, via a sequence of the hypothesis testing, the possible faults in the FF/CC control system can be examined. The current operation performance is compared to the one that would be obtained by using a minimum achievable variance controller. As long as the value of the test statistics exceeds the threshold value, the effect of the just-identified fault is eliminated. It can systemati-

cally identify and isolate the system that contains the possible fault information. This is a stepwise diagnosis procedure. Without a detailed familiarity with the model of the dynamic system being supervised, the proposed measurements-driven based method is the accurate fault identification in the operation system. In addition, it is possible for several different types of diagnosed faults to occur simultaneously, and virtually the proposed method can be used to characterize them. This prototype is used to verify the numerical simulation testing in this paper. The assumption of the disturbance with the uncorrelated noises has a limitation for practical consideration. The work for the correlated noise will be considered at our next stage. Moreover, an extended research on assessing robustness for industrial applications will be further studied in the future.

## ACKNOWLEDGMENTS

This work is partly sponsored by the Ministry of Economic Affairs, R.O.C. and the Center-of-Excellence Program on Membrane Technology, the Ministry of Education, Taiwan, R.O.C.

## REFERENCES

1. Y. Yea and J. Chen, *Ind. Eng. Chem. Res.*, **44**, 5660 (2005).
2. Y. Yea and J. Chen, *American control conference*, Portland, Oregon (2005).
3. B. Huang and S. L. Shan, *Performance assessment of control loops: theory and applications*, Springer-Verlag; London (1999).
4. L. Desborough and T. J. Harris, *Can. J. Chem. Eng.*, **70**, 1186 (1992).
5. L. Desborough and T. J. Harris, *Can. J. Chem. Eng.*, **71**, 605 (1993).
6. B.-S. Ko, T.-F. Edgar and J. Lee, *Korean J. Chem. Eng.*, **21**, 1 (2004).
7. S. Lee, S. Yeom and K.-S. Lee, *Korean J. Chem. Eng.*, **21**, 575 (2004).
8. B.-S. Ko and T. F. Edgar, *AIChE J.*, **46**, 281 (2000).
9. J. Chen, S.-C. Huang and Y. Yea, *J. Chem. Eng. Jpn.*, **38**, 181 (2005).
10. N. Stanfelj, T. E. Marlin and J. F. Macgregor, *Ind. Eng. Chem. Res.*, **32**, 301 (1993).
11. N. F. Thornhill, J. W. Cox and M. A. Paulonis, *Control Engineering Practice*, **11**, 1481 (2003).
12. W. X. Zheng and C. B. Feng, *Automatica*, **26**, 769 (1990).
13. G. Jacovitti and G. Scarano, *IEEE Trans. on Acoustics, Speech and Signal Processing*, **41**, 525 (1993).
14. D. M. Etter and S. D. Stearns, *IEEE Transactions on ASSP*, **29**, 582 (1981).
15. D. C. Montgomery and G. C. Runger, *Applied statistics and probability for engineers*, 3rd Edition, John Wiley & Sons, Inc. (2003).
16. B.-S. Ko and T. F. Edgar, *Assessment of achievable PI control performance for linear process with dead time*, Proceedings of ACC, Philadelphia (1998).
17. C. B. Lynch and G. A. Dumount, *IEEE Trans. on Control System Technology*, **4**, 185 (1996).